WEP Warwick Evans Publishing

International Journal of Natural Resources and Environmental Studies

ISSN: 3006-2012 (Print), ISSN: 3006-0834 (Online) | Volume 8, Number 4, Year 2026
DOI: https://doi.org/10.62051/ijnres.v8n4.12
Journal homepage: https://wepub.org/index.php/IJNRES/index

Failure Characteristics of Anchorage Structure After Cylindrical Reaming

Aolong Liu*

School of Energy Science and Engineering, Henan Polytechnic University, Jiaozuo 454003, China.
*Corresponding Author: Aolong Liu (Email: 2042543424@qq.com)

ABSTRACT

To reveal the failure mechanism of anchorage systems with cylindrical reaming and clarify the internal correlation among anchorage failure, surrounding rock stress, and anchorage agent displacement, a three-dimensional integrated model of the surrounding rock-bolt-anchoring agent-reaming section was established using the Abaqus numerical simulation method based on the cylindrical reaming anchorage engineering in deep soft rock roadways. Seven groups of working conditions with different reaming diameters were designed. Combined with visual analysis of surrounding rock stress and anchorage agent displacement nephograms, as well as theoretical calculations, the failure characteristics, types, and evolution laws of the anchorage structure after reaming were systematically studied. The results show that anchorage failure in cylindrical reaming is dominated by damage to the anchoring agent, which manifests in three core forms: interfacial debonding, plastic rheology, and fracture. An unreasonable reaming diameter causes significant stress concentration at the junction of the reaming section and the reference borehole, and the degree of stress concentration has a nonlinear relationship with the reaming diameter, which is the core inducement of anchorage failure. The displacement and deformation of the anchoring agent increase with the deviation of the reaming diameter from the optimal value, and the deformation concentration area is highly coincident with the stress concentration area, which directly determines the type and degree of anchorage failure. The optimal reaming diameter is 40 mm. Under this condition, the surrounding rock stress is uniformly distributed, the displacement and deformation of the anchoring agent are the smallest, and the risk of anchorage failure is the lowest. The research results provide an intuitive theoretical basis for parameter optimization and failure prevention and control of cylindrical reaming anchorage technology.

KEYWORDS

Reaming support; Anchorage failure; Soft rock roadway; Numerical simulation.

1. INTRODUCTION

As coal mining in China continues to deepen, the surrounding rock of deep roadways generally exhibits low strength, high rheology, high stress, and weak cementation. As the core technology for controlling surrounding rock stability, the reliability of anchorage support directly determines the long-term safety and efficient production of roadways [1,2]. Cylindrical reaming anchorage can optimize the interfacial stress state and improve anchorage stiffness and ultimate bearing capacity, making it a key technical direction for high-efficiency support of deep soft rock roadways [3,4]. However, the lack of a mechanical basis for selecting the reaming diameter often leads to failures such as debonding, shear rheology, and overall fracture of the anchoring agent, which seriously restricts the large-scale popularization of the technology [5]. Many studies have shown that anchorage failure is essentially the result of the combined effect of surrounding rock stress concentration and

uncoordinated deformation of the anchoring agent. Surrounding rock stress nephograms and anchoring agent displacement nephograms can intuitively reveal the evolution laws of the stress and displacement fields, providing visual support for failure mechanism analysis [6].

At present, scholars at home and abroad have conducted extensive research on reaming parameters, anchorage mechanical properties, and interfacial failure mechanisms. Jing et al. [7] revealed the entire process of anchorage behavior, from elastic deformation and interfacial debonding to plastic failure, through pull-out tests. Cheng et al. [8] conducted mechanical tests on reamed anchorage in weak coal and rock masses, confirming that reaming can significantly improve the stress state of the anchorage. Meng et al. [9] studied the interaction mechanism between surrounding rock and bolt-shotcrete support in deep, soft-rock roadways, emphasizing the influence of interfacial coordinated deformation on support stability. Guan et al. [10] analyzed the damage evolution of anchored surrounding rock by numerical simulation, providing a methodological reference for anchorage failure identification. Hao et al. [11] verified the positive effect of reaming on improving anchorage force through field tests, but did not systematically clarify the regulatory mechanism by which reaming diameter affects stress distribution, deformation coordination, and failure mode. Overall, existing studies mostly focus on the influence of reaming parameters on anchorage force, lacking a whole-process visual analysis of anchorage failure. In addition, stress or displacement nephograms are often used separately, failing to organically combine stress concentration, deformation accumulation, and failure evolution path, so it is difficult to accurately reveal the internal correlation between reaming diameter and anchorage failure.

Therefore, this paper takes the surrounding rock stress nephogram and anchoring agent displacement nephogram as the core analysis methods, and establishes a three-dimensional integrated model of the surrounding rock-bolt-anchoring agent by Abaqus. The stress distribution, deformation characteristics, and failure evolution law of the anchorage system under different reaming diameters are systematically studied, the optimal reaming parameters are clarified, and prevention and control measures are proposed. The research results can provide a theoretical basis and technical reference for the design and engineering application of reaming anchorage in deep soft rock roadways.

2. NUMERICAL SIMULATION SETUP

2.1. Engineering Background

This research is based on the cylindrical reaming anchorage project of the 3# coal seam soft rock roadway in a deep coal mine. The buried depth of the roadway is 1150 m, and the surrounding rock is mainly argillaceous shale with a saturated compressive strength of 8.2–12.5 MPa. It belongs to a typical deep high-stress soft rock stratum with developed fractures, poor cementation, and susceptibility to plastic rheology and collapse failure.

2.2. Numerical Simulation Scheme

The Abaqus/Standard implicit solver was used to construct an integrated three-dimensional numerical model of surrounding rock, bolt, anchoring agent, and reaming section to simulate the evolution characteristics of surrounding rock stress and anchoring agent displacement during bolt pull-out, providing reliable support for the acquisition and analysis of surrounding rock stress nephograms and anchoring agent displacement nephograms.

2.2.1. Model Establishment and Parameter Setting

The model size was reasonably determined according to engineering practice and numerical simulation accuracy. The surrounding rock adopts a cylindrical model with a diameter of 300 mm and a height of 30 mm, with fixed constraints at the bottom and the Mohr-Coulomb plastic criterion to fit the plastic rheological characteristics of soft rock. The bolt is made of HRB400E deformed steel

bar with a diameter of 20 mm and a length of 300 mm, adopting a linear elastic constitutive model. The anchoring agent adopts CK2360 resin anchoring agent, whose thickness is adjusted synchronously with the reaming diameter, and a bond-slip model is used to simulate the debonding failure of the interface between the anchoring agent, bolt, and surrounding rock.

2.2.2. Working Condition Setting

One control working condition and six groups of different reaming diameter working conditions were set, namely 24 mm (reference borehole diameter), 30 mm, 40 mm, 50 mm, 60 mm, 70 mm, and 80 mm. Three parallel models were set for each working condition, and the calculation error was strictly controlled within ±3% to ensure the reliability of the test results. Displacement-controlled loading was adopted, with 5 mm axial displacement applied at the top of the bolt at a loading rate of 0.01 mm/s to simulate the whole process of bolt pull-out. The surrounding rock stress nephograms and anchoring agent displacement nephograms at the peak pull-out moment were mainly extracted to provide sufficient data support for the subsequent anchorage failure analysis,the modeling is shown in Figure 1.

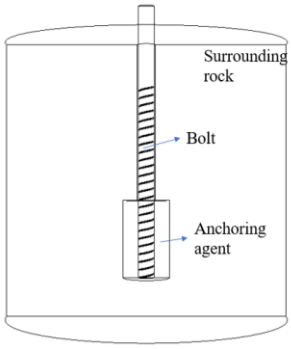

Figure 1. Schematic of Numerical Simulation Model

3. ANALYSIS OF ANCHORAGE FAILURE CHARACTERISTICS BASED ON NUMERICAL SIMULATION

3.1. Analysis of Surrounding Rock Stress Nephogram and Its Correlation with Anchorage Failure

The surrounding rock stress nephogram can intuitively present the stress distribution and stress concentration characteristics of the surrounding rock under different reaming diameters, and stress concentration is the core inducement of anchorage failure. By comparing the Mises stress nephograms of the surrounding rock under seven working conditions, the stress distribution law and its correlation with anchorage failure are analyzed as follows.

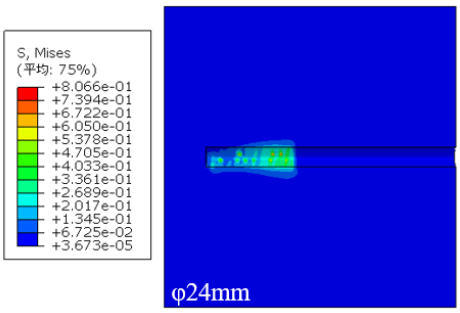

Figure 2. Stress nephogram of non-reaming condition

It can be seen from Fig. 2 that the borehole wall section of the 24 mm reference non-reaming anchorage structure is smooth without size mutation, the overall stress distribution of the surrounding

rock is relatively uniform, and there is no significant local stress concentration area. The interfacial stress is gentle and uniform under pull-out load, and the main failure mode of the anchorage system under this working condition is the interfacial debonding between the anchoring agent and the surrounding rock.

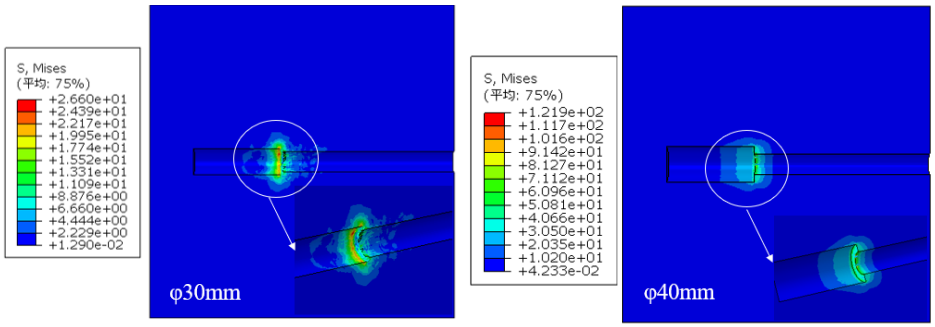

Figure 3. Stress nephograms of small-diameter reaming (30 mm, 40 mm)

It can be seen from Fig. 3 that when the reaming diameter is 30 mm, the section mutation at the junction of the reaming section and the reference non-reaming section is significant, the surrounding rock stress distribution is extremely uneven, and the local stress concentration is obvious. The high stress is mainly concentrated at the aperture junction and the periphery of the orifice. The concentrated stress causes plastic damage to the surrounding rock and leads to the anchorage interface, resulting in interfacial stress overload and finally inducing the interfacial debonding failure between the anchoring agent and the surrounding rock. Under the 40 mm reaming condition, the transition between the reaming section and the original borehole wall is gentle and smooth, with no obvious abrupt interface. The overall surrounding rock stress distribution is uniform and reasonable, with no significant local stress concentration. The overall stress level is moderate and matches the mechanical strength of the surrounding rock. The load transfer path is smooth and stable, and the plastic damage range of the surrounding rock is small, which can form a stable and effective confining pressure constraint on the anchoring agent, effectively avoiding local stress overload of the anchoring agent, and significantly reducing the risk of anchorage failure.

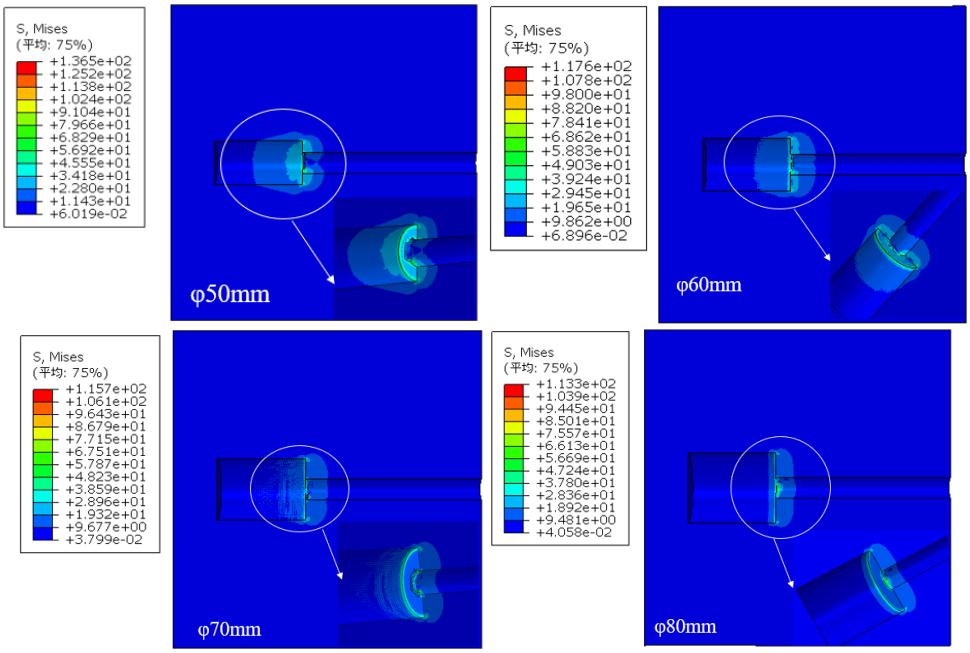

Figure 4. Stress nephograms of large-diameter reaming (50–80 mm)

It can be seen from Fig. 4 that as the reaming diameter continues to increase to the range of 50–80 mm, the disorder degree of surrounding rock stress distribution continues to intensify, the stress concentration phenomenon is significantly enhanced, and the scope of the high stress concentration area continues to expand, extending from the aperture junction to the deep surrounding rock. The excessive reaming diameter causes large-scale plastic damage and even penetration of the plastic zone in the surrounding rock, destroying the bearing integrity of the rock mass. It can no longer provide a stable confining pressure constraint for the anchoring agent, resulting in excessive axial shear load on the anchoring agent, and then plastic deformation or even structural fracture occurs.

In summary, the reaming diameter has an obvious nonlinear relationship with the degree of surrounding rock stress concentration, surrounding rock damage, and anchorage failure risk. 40 mm is the optimal reaming diameter, with a gentle interface transition, uniform stress distribution, and optimal bearing performance. The farther the reaming diameter deviates from the optimal value of 40 mm, whether it is the small-diameter reaming of 30 mm or the large-diameter reaming of 50–80 mm, different degrees of stress concentration and surrounding rock damage will be induced, and the risk of premature failure of the anchorage structure will increase accordingly.

3.2. Analysis of Anchoring Agent Displacement Nephogram and Its Correlation with Anchorage Failure

The displacement nephogram of the anchoring agent can intuitively present the displacement deformation distribution, deformation amount, and concentration area of the anchoring agent under different reaming diameters. The magnitude and distribution of displacement deformation directly determine the type and degree of anchorage failure. By comparing the displacement nephograms of the anchoring agent under seven working conditions, the displacement deformation law and its correlation with anchorage failure are analyzed as follows (since the applied displacement load direction is the negative direction of the Z-axis, the values in the nephograms are negative)

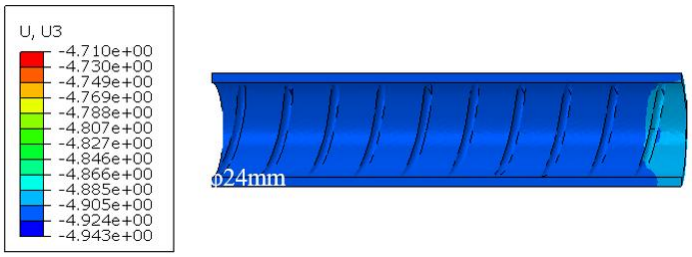

Figure 5. Displacement nephogram of anchoring agent under non-reaming conditions

It can be seen from Fig. 5 that under the 24 mm non-reaming reference condition, the axial deformation distribution of the anchoring agent shows good uniformity, with a displacement range of 4.710–4.943 mm. There is no local deformation concentration or singular distortion in the whole section, and the deformation amount presents a gentle gradient transition along the axial direction of the bolt. This uniform deformation characteristic originates from the uniform load transfer along the entire length of the anchorage interface, resulting in coordinated overall deformation of the structure, which is consistent with the distribution law of "uniform dispersion along the entire length and no local stress concentration" shown in the surrounding rock stress nephogram.

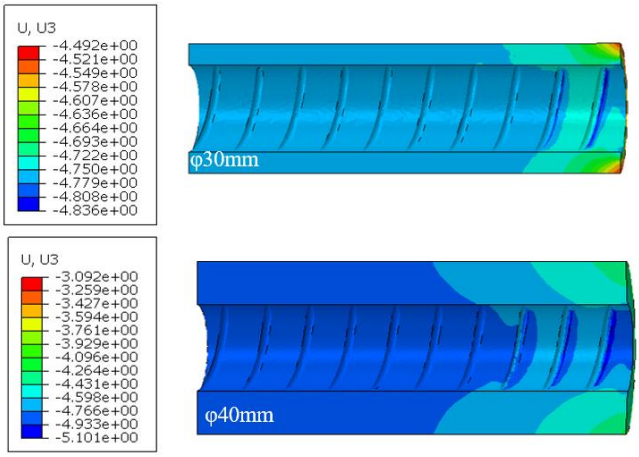

Figure 6. Displacement nephograms of anchoring agent under reaming diameters (30 mm, 40 mm)

It can be seen from Fig. 6 that under the 30 mm and 40 mm reaming conditions, the axial displacement ranges of the anchoring agent are 4.492–4.836 mm and 3.092–5.101 mm, respectively. For the 30 mm reaming structure, the interface section mutation is obvious, and the deformation of the anchoring agent is concentrated at the aperture junction. Affected by the constraint and inhibition of the surrounding rock in the reaming section, the axial deformation partition of the anchoring agent is significant, forming an obvious displacement boundary at the junction, corresponding to the surrounding rock stress concentration distribution characteristics. For the 40 mm reaming structure, the interface transition is gentle, the deformation of the anchoring agent presents a gentle gradient transition along the axial direction, and the displacement interface shows a "bottle" shape distribution. The surrounding rock constraint makes the deformation in the thread area significant, the interface displacement boundary is clear, the overall shape of the anchoring agent is intact without obvious structural distortion, and the comprehensive bearing effect is optimal.

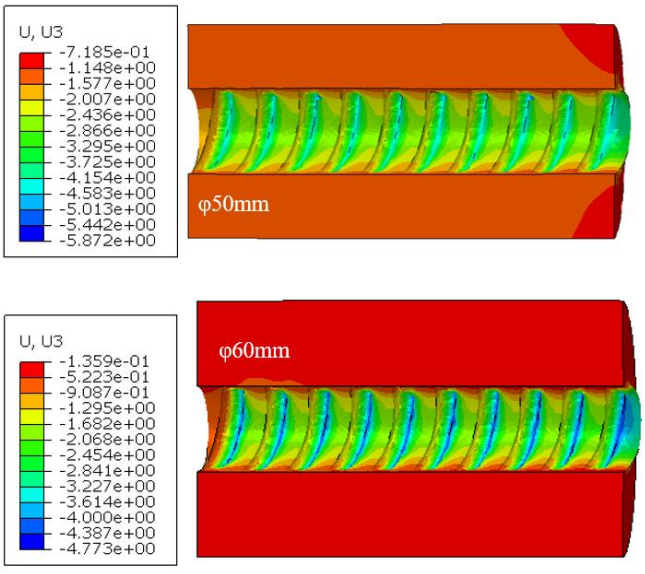

Figure 7. Displacement nephograms of anchoring agent under reaming diameters (50 mm, 60 mm)

It can be seen from Fig. 7 that under the 50 mm and 60 mm reaming conditions, the axial displacement ranges of the anchoring agent are 0.719–5.872 mm and 0.136–4.773 mm, respectively. For the 50 mm reaming structure, the interface mutation degree is significantly intensified, and the deformation difference of the anchoring agent is highly concentrated in the inner area of the reaming section. Affected by the constraint and inhibition of the surrounding rock in the reaming section, the axial deformation partition of the anchoring agent is significant, and obvious plastic deformation begins to appear. A large-scale displacement boundary area is formed at the junction of the reaming section

and the reference section, which corresponds to the distribution law of large-scale extension and expansion of the high-stress area in the surrounding rock nephogram. For the 60 mm reaming structure, the interface difference continues to increase, the axial deformation inhomogeneity of the anchoring agent is further improved, and the diffusion range of the displacement boundary continues to expand. Affected by the constraint and inhibition of the surrounding rock, the overall deformation and distortion of the anchoring agent intensify, the structural integrity is obviously damaged, and the overall bearing performance is significantly deteriorated.

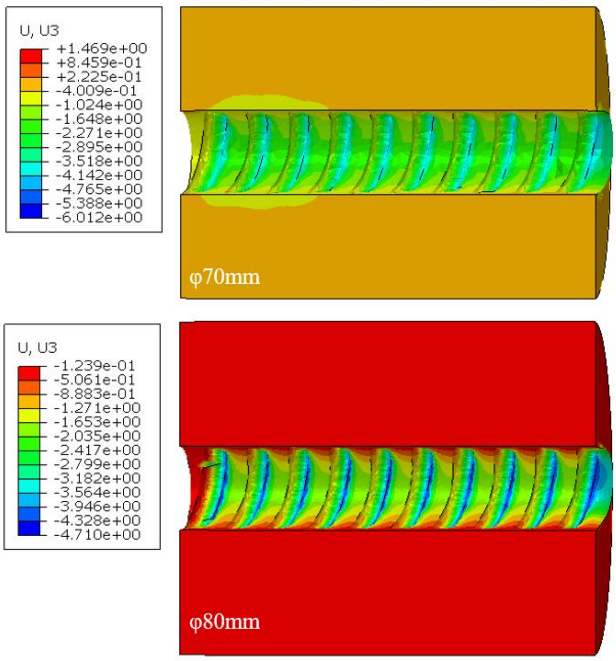

Figure 8. Displacement nephograms of anchoring agent under large-diameter reaming (70–80 mm)

It can be seen from Fig. 8 that under the 70 mm and 80 mm reaming conditions, the axial displacement ranges of the anchoring agent are - 1.469–6.012 mm and 0.124–4.710 mm, respectively. For the 70 mm reaming structure, the interface mutation degree is significantly increased, the deformation of the anchoring agent is further intensified, and even reverse displacement occurs locally. The axial deformation partition of the anchoring agent is disordered, and the displacement boundary area is diffuse and irregular, which corresponds to the law of disordered stress distribution and large-scale penetration of plastic damage in the surrounding rock nephogram. For the 80 mm super-large reaming structure, the interface difference reaches the maximum in the whole series, the local deformation of the anchoring agent is highly concentrated, the overall deformation uniformity is extremely poor, the surrounding rock constraint effect is basically invalid, the structural distortion and damage of the anchoring agent are serious, and it is difficult to maintain stable and effective anchorage bearing.

In summary, the surrounding rock stress distribution and anchoring agent deformation characteristics of anchorage structures with different reaming diameters are highly coupled, and both show obvious nonlinear variation laws with reaming size. 40 mm is the optimal reaming diameter, with a gentle interface transition, uniform surrounding rock stress distribution, gentle and coordinated deformation of the anchoring agent, good structural integrity, and optimal overall bearing performance. The farther the reaming diameter deviates from the optimal value, whether it is small-diameter under-reaming or large-diameter over-reaming, significant interfacial stress concentration and local deformation abnormality of the anchoring agent will be induced, the surrounding rock constraint capacity continues to deteriorate, the structural plastic damage intensifies, and the risk of anchorage failure increases significantly.

4. EVOLUTION LAW OF ANCHORAGE FAILURE AND PREVENTION & CONTROL TECHNICAL MEASURES

4.1. Evolution Law of Anchorage Failure

Combined with the spatial-temporal evolution characteristics of surrounding rock stress nephograms and anchoring agent axial displacement nephograms under each reaming diameter condition, as well as the dynamic monitoring data of stress and displacement during the whole pull-out process, the failure evolution law of cylindrical reaming anchorage structure can be systematically clarified. The whole failure process follows the chain evolution path of local stress concentration of surrounding rock → stress overload of anchoring agent → local debonding of anchorage interface → accumulation of anchoring agent displacement deformation → material plastic rheology → overall structural fracture failure. The evolution process rate and final failure mode are highly related to the reaming diameter parameters. The specific evolution characteristics of each size condition are as follows:

Small-diameter reaming (30 mm) and original non-reaming (24 mm) conditions: The anchorage failure evolution process of such conditions is slow. The original 24 mm non-reaming structure has no size mutation at the interface, uniform overall stress distribution and gentle coordinated deformation of the anchoring agent, only uniform interfacial debonding occurs along the entire length, without subsequent plastic damage evolution. For the 30 mm small-diameter reaming structure, the stress concentration is limited only to the interface between the reaming section and the reference borehole, the local deformation difference of the anchoring agent is limited, and the failure starts from local interfacial debonding. The overall deformation amount is small, and the stress concentration degree is low, so it is difficult to further induce plastic rheology and structural fracture of the anchoring agent. The failure mode is mainly interfacial debonding, which is consistent with the mechanical characteristics of low surrounding rock stress concentration and gentle uniform deformation of the anchoring agent.

Optimal reaming diameter (40 mm) condition: There is no significant chain failure evolution process in the anchorage system under this size. The interface size transition is gentle, the overall surrounding rock stress distribution is uniform without obvious concentration, the axial deformation of the anchoring agent is small and evenly distributed along the entire section, and the interface bonding state is stable and reliable. Only local slight interfacial debonding occurs under ultimate pull-out load; the overall stress and displacement are in a stable and controllable range throughout the process, the risk of anchorage failure is extremely low, and the comprehensive bearing performance is optimal.

Large-diameter and super-large-diameter reaming (50–80 mm) conditions: The anchorage failure evolution process of such conditions is significantly accelerated. With the gradual increase of pull-out load, the scope of high stress concentration in the surrounding rock continues to expand, and the stress peak continues to rise, firstly causing stress overload at the anchoring agent interface and inducing overall interfacial debonding. Then, the uneven deformation of the anchoring agent continues to accumulate, the internal shear damage continues to develop, and plastic rheology gradually occurs. When the local stress exceeds the shear strength of the anchoring agent and the displacement deformation reaches the limit threshold, the overall shear fracture failure of the structure finally occurs. The farther the reaming diameter deviates from the optimal size, the faster the failure evolution rate and the more serious the structural damage degree, which is highly coupled with the law of intensified surrounding rock stress concentration, disordered deformation, and increased displacement range of the anchoring agent.

4.2. Technical Measures for Anchorage Failure Prevention and Control

Based on the evolution law of surrounding rock stress and anchoring agent displacement and the internal mechanism of anchorage failure analyzed above, combined with the actual application

requirements of engineering sites, with the core prevention and control principles of balancing surrounding rock stress distribution, inhibiting abnormal deformation of anchoring agent, and strengthening interfacial bonding bearing performance, and combined with the engineering application characteristics of the rapid reaming anchorage technology of Chengdu Institute of Mining Engineering, the following systematic and targeted prevention and control technical measures are proposed:

The optimal reaming diameter of 40 mm is preferred, which can effectively alleviate the section mutation effect at the junction of the reaming section and the original reference borehole, balance the surrounding rock stress field, optimize the axial shear stress distribution of the anchoring agent, reduce the overall displacement and deformation of the anchoring agent, and curb the risk of anchorage failure from the parameter source. The super-large reaming parameter of 80 mm is strictly prohibited in engineering applications; the large-diameter reaming of 60–70 mm should be carefully selected. If it is really necessary to adopt under engineering conditions, special mechanical safety verification must be carried out to ensure that the peak stress of the anchoring agent is always lower than the allowable shear strength of the material.

During the on-site construction stage, the floating slag, mud skin on the borehole wall, and rust impurities on the bolt surface must be thoroughly cleaned to ensure the full filling and uniform mixing of the anchoring agent, improve the interfacial bonding strength between the bolt-anchoring agent and anchoring agent-surrounding rock, and inhibit the early debonding failure from the interface level. For the over-reaming condition of 50 mm and above, the borehole wall grouting reinforcement modification process is implemented to improve the overall mechanical strength and confining pressure constraint capacity of the surrounding rock, alleviate the local stress concentration, and block the accumulation and development of plastic deformation of the anchoring agent.

Resin anchoring materials with excellent shear failure resistance, plastic rheology resistance, and long-term creep deformation resistance are selected. CK2360 and above standard anchoring agents are preferred in engineering to improve the shear strength and deformation resistance of the anchoring agent itself, resist the accumulation of deformation damage under long-term axial shear load, and delay the overall failure evolution process of the anchorage system.

Combined with the construction characteristics of the rapid reaming drilling equipment of Chengdu Institute of Mining Engineering, optimize the on-site reaming construction technology, strictly control the reaming forming accuracy, ensure the uniform transition of the reaming section aperture, and avoid the secondary stress concentration caused by construction size deviation. At the same time, improve the professional training of construction personnel, standardize the whole construction process, such as bolt installation and anchoring agent mixing time and uniformity control, and eliminate the non-mechanical anchorage failure caused by various construction defects.

5. CONCLUSIONS

The failure of the cylindrical reaming anchorage system is dominated by the damage evolution of the anchoring agent itself, which is mainly divided into three failure modes: interfacial debonding, material plastic rheology, and structural shear fracture. The occurrence conditions, evolution process, and final form of each failure mode are highly related to the reaming diameter parameters, the degree of surrounding rock stress concentration, and the displacement and deformation characteristics of the anchoring agent. The deformation concentration area of the anchoring agent is highly coincident with the high stress concentration area of the surrounding rock in space, which is the core control area of anchorage structure failure.

1. The visual analysis of surrounding rock stress nephograms shows that there is a significant nonlinear correlation between reaming diameter and the degree of surrounding rock stress concentration. Within the scope of the research conditions, 40 mm is the optimal reaming diameter,

under which the surrounding rock stress field is uniformly distributed without significant local stress concentration. The original non-reaming of 24 mm, small-diameter reaming of 30 mm, and large-diameter reaming of 50 mm and above will induce different degrees of local stress concentration. The farther the reaming size deviates from the optimal value of 40 mm, the more significant the surrounding rock stress concentration effect and the wider the plastic damage range.

2. The visual analysis of anchoring agent axial displacement nephograms shows that the deformation characteristics of the anchoring agent also present a nonlinear response law with the reaming diameter. Under the optimal 40 mm condition, the overall displacement of the anchoring agent is the smallest, and the deformation distribution along the entire section is the most uniform and coordinated. The deformation of small-diameter reaming is concentrated at the aperture interface, which is easy to induce early interfacial debonding failure. The deformation distribution of large-diameter reaming is disordered, and the displacement range is significantly increased; the internal shear damage accumulates rapidly, and it is easy to develop into plastic rheology and overall fracture failure, which is highly coupled with the deterioration law of the surrounding rock stress distribution.

3. The failure of reaming anchorage structure follows the chain evolution path of surrounding rock stress concentration → anchoring agent stress overload → interfacial local debonding → continuous accumulation of displacement deformation → material plastic rheology → overall fracture failure. The farther the reaming size deviates from the optimal parameter of 40 mm, the faster the failure evolution rate and the more serious the structural damage. The comprehensive prevention and control measures proposed in this study, such as optimizing reaming parameters, improving interfacial bonding quality, selecting high-performance materials, and standardizing construction procedures, can effectively balance stress distribution, inhibit abnormal deformation, delay the failure process, and significantly improve the overall stability of the anchorage system.

REFERENCES

[1] Xie H P. Research progress of deep rock mechanics and mining theory[J]. Journal of China Coal Society, 2019, 44(5): 1283-1305.

[2] Ning Y G, Ma S W, Cao C. Anchorage failure analysis and support countermeasures of deep mining roadway[J]. Coal Science and Technology, 2021, 49(8): 23-29.

[3] Cheng L X. Parameter optimization analysis and mechanical property test of anchorage based on reaming[J]. Safety in Coal Mines, 2023, 54(7): 196-204.

[4] Zhang H, Li G S, Su F Q. Numerical analysis of mechanical characteristics of bolt hole bottom reaming in weak coal and rock roadway based on ABAQUS[J]. Journal of Henan Polytechnic University (Natural Science), 2019, 38(1): 13-18.

[5] He D Y, Liu S W, Fu M X, et al. Guarantee method and experiment of anchorage effect in bottom reaming area of coal mine weak surrounding rock anchorage hole[J]. Journal of China Coal Society, 2024, 49(S1): 108-120.

[6] Li P F, Huang J L, Wang F. Whole process and influencing factors of progressive failure of bolt under pull-out load[J]. Journal of Beijing University of Technology, 2021, 47(4): 346-356.

[7] Jing H W, Yin Q, Zhu D, et al. Experimental study on the whole process of instability and failure of the surrounding rock anchorage structure in deep roadway[J]. Journal of China Coal Society, 2020, 45(3): 889-901.

[8] Cheng L X, Zhang H, Jiang P F, et al. Mechanical characteristics and experimental study of reaming anchorage in weak coal and rock mass[J]. Journal of Mining & Safety Engineering, 2019, 36(6): 1153-1160.

[9] Meng Q B, Song Z M, Liu B, et al. Interaction between surrounding rock and bolt-shotcrete U-steel support in deep soft rock roadway[J]. Coal Science and Technology, 2024, 52(7): 23-36.

[10] Guan K, Jiang X, Zhu W C, et al. Numerical simulation study on damage failure and anchorage timing of anchored surrounding rock in a middle roadway of Xincheng Gold Mine[J]. China Mining Magazine, 2026, 35(1): 156-164.

[11] Hao F S, Qi Y J. Experimental study on bolt reaming technology and anchorage force[J]. Journal of China Coal Society, 2008, 33(12): 1358-1361